MOLECULAR AND CELLULAR BIOLOGY, Dec. 2003, p. 8405–8415 Vol. 23, No. 23
0270-7306/03/$08.00+0 DOI: 10.1128/MCB.23.23.8405–8415.2003

A Novel Set of Nuclear Localization Signals Determine Distributions of the αCP RNA-Binding Proteins

Alexander N. Chkheidze and Stephen A. Liebhaber*

Departments of Genetics and Medicine, University of Pennsylvania School of Medicine, Philadelphia, Pennsylvania 19104

Received 10 June 2003/Returned for modification 22 July 2003/Accepted 29 August 2003

αCPs comprise a subfamily of KH-domain-containing RNA-binding proteins with specificity for C-rich pyrimidine tracts. These proteins play pivotal roles in a broad spectrum of posttranscriptional events. The five major αCP isoforms are encoded by four dispersed loci. Each isoform contains three repeats of the RNA-binding KH domain (KH1, KH2, and KH3) but lacks other identifiable motifs. To explore the complexity of their respective functions, we examined the subcellular localization of each αCP isoform. Immunofluorescence studies revealed three distinct distributions: αCP1 and αCP2 are predominantly nuclear with specific enrichment of αCP1 in nuclear speckles, αCP3 and αCP4 are restricted to the cytoplasm, and αCP2-KL, an αCP2 splice variant, is present at significant levels in both the nucleus and the cytoplasm. We mapped nuclear localization signals (NLSs) for αCP isoforms. αCP2 contains two functionally independent NLS. Both NLSs appear to be novel and were mapped to a 9-amino-acid segment between KH2 and KH3 (NLS I) and to a 12-amino-acid segment within KH3 (NLS II). NLS I is conserved in αCP1, whereas NLS II is inactivated by two amino acid substitutions. Neither NLS is present in αCP3 or αCP4. Consistent with mapping studies, deletion of NLS I from αCP1 blocks its nuclear accumulation, whereas NLS I and NLS II must both be inactivated to block nuclear accumulation of αCP2. These data demonstrate an unexpected complexity in the compartmentalization of αCP isoforms and identify two novel NLS that play roles in their respective distributions. This complexity of αCP distribution is likely to contribute to the diverse functions mediated by this group of abundant RNA-binding proteins.

Posttranscriptional controls play a major role in the regulation of eukaryotic gene expression (24, 65). These controls (i) can increase the complexity of nuclear RNAs via alternative splicing and editing, (ii) can modulate information flow from the nucleus to cytoplasm, and (iii) can alter levels and sites of protein synthesis via controls over mRNA stability, translation efficiency, and subcellular localization (4, 56, 68). RNA-binding proteins that mediate these controls can be categorized based on the presence of one or more conserved RNA-binding motifs (for reviews, see references 6 and 37). The sequence specificity of these proteins, the identities of their RNA targets, and the respective mechanisms of action are therefore of significant interest.

Studies from our laboratory and others have focused on the structures and actions of a subfamily of RNA-binding proteins, the αCPs (31, 39). These proteins, also referred to as PCBPs (17) and hnRNP Es (34, 58), contain a triplication of the KH domain (43, 69). The 70-amino-acid KH domain comprises a triple-β-sheet platform supporting three α-helical segments (35, 36, 50, 51). Cocrystal structures reveal that the KH domain can interact in a highly specific manner with four to five contiguous bases in a target RNA (5, 27). Two KH domain subtypes have been identified: the type 1 KH domain (e.g., KH3 of hnRNP K) has a C-terminal βα extension, and the type 2 KH domain (e.g., ribosomal protein S3) contains an N-terminal αβ extension (21). The KH domains in the αCPs are type 1 (40). KH domains are often represented in proteins in multiple copies. Since each KH domain has the potential to independently interact with a target RNA sequence, the complexity and specificity of RNA interaction for these proteins can be quite high (66, 74; our unpublished data).

Our laboratory has focused on the role of αCPs in mRNA stabilization. These studies have defined a cytosine (C)-rich *cis*-acting stability element within the 3′ untranslated region (UTR) of the human (h) α-globin mRNA that serves as a binding site for αCP both in vitro and in vivo (28, 32, 83). Studies in our laboratory and others have identified closely related αCP binding sites in the 3′ UTRs of additional highly stable mRNAs (7, 10, 25, 61, 72, 86). In the case of the hα-globin mRNA, the RNP "α-complex" in the 3′ UTR appears to represent a 1:1 interaction of αCP with the C-rich motif (8), although there is evidence that additional proteins may also bind at this site (30, 63, 84, 85). These data suggest that the α-complex may represent a widely distributed and general determinant of mRNA stabilization (25).

The αCPs involved in α-complex assembly can represent several isoforms (8, 31, 39). Whether these various αCP isoforms are performing unique functions or are redundant in their actions is not known. The functions mediated by αCP RNP complexes are in fact quite diverse (for review, see reference 41). As mentioned above, assembly of the 3′ UTR α-complex in α-globin mRNA mediates mRNA stabilization (32, 82, 83). This stabilization may reflect direct steric protection of the 3′ UTR from endonucleolytic attack (79), and/or it may reflect protection of the poly(A) tail from rate-limiting decay via interactions in *cis* between the bound αCP and the poly(A)-binding protein (30, 49, 78). αCPs also mediate translational controls. An array of αCP binding sites within the 3′ UTR of the 15-lipoxygenase mRNA has been linked to devel-

* Corresponding author. Mailing address: Rm. 428, Clinical Research Building, 415 Curie Blvd., Philadelphia, PA 19104. Phone: (215) 898-7834. Fax: (215) 573-5157. E-mail: Liebhabe@mail.med.upenn.edu.

opmentally regulated translational repression during erythroid maturation (56–58). In contrast, association of αCP with the 5′ UTR of the polio viral RNA serves as an enhancer of internal ribosome entry site-mediated translation (2, 3). αCP binding within the 3′ UTR has also been implicated in the activation of maternal mRNA translation in early embryonic development in *Xenopus* via control of cytoplasmic polyadenylation (59). Additional systems are reported to involve αCP binding in the control of various aspects of mRNA expression (63, 84, 85; reviewed in reference 41). Thus, the targets and actions of the αCPs are quite diverse and may reflect the actions of one or more of the defined αCP isoforms.

αCP isoforms are encoded by four unlinked loci in the human and mouse genomes: *PCBP1*, *PCBP2*, *PCBP3*, and *PCBP4* (38, 39, 75) (see also Fig. 1, left). Each locus has been mapped, sequenced, and characterized for mRNA structure (38, 39). A total of five major αCP isoforms have been identified in human or mouse tissues: αCP1, αCP2, αCP3, αCP4, and a major αCP2 splice variant, αCP2-KL, that differs from αCP2 by the exclusion of a 31-amino-acid segment in the region between the KH2 and KH3 encoded by a single exon (exon 8a) (17, 38, 39). These proteins are broadly expressed in human and mouse tissues and demonstrate polyC-binding specificity (34, 38, 39; unpublished observations). αCP1 and αCP2 share the highest level of amino acid sequence similarity at 89% (75), αCP3 is more divergent, and αCP4 is the most distantly related (52% divergence from αCP2 [39]). Each protein contains three similarly spaced KH domains; two KH repeats are located in the N terminus followed by a nonconserved region of variable length, and the third KH domain is located at the C terminus. Posttranslational modifications may regulate the binding of αCPs to RNA. For example, phosphorylation of αCP1 and αCP2 results in a marked decrease in RNA-binding activity (34). An additional major determinant of αCP isoform function may relate to subcellular localization. Although the defined roles of αCP in mRNA stability and translational control suggest a cytoplasmic localization, prior attempts to sublocalize αCPs did not resolve the question of whether αCP is in fact nuclear or cytoplasmic (17, 18).

Protein transport from cytoplasm to nucleus is mediated by multiple families of soluble factors. It is generally accepted that nuclear proteins carry a nuclear localization signal (NLS) (11, 45, 53, 67). NLSs vary considerably from relatively short stretches of residues to large protein domains with relaxed sequence conservation. Although different in structure, NLSs all seem to play the same role: recognition by soluble factors that mediate transport through the nuclear pore complexes (19, 20, 42, 54, 55, 77).

In the present study each of the five major isoforms was individually assessed for subcellular localization, and the signals underlying their nuclear versus cytoplasmic distribution were defined. These data demonstrate an unexpected complexity in αCP isoform compartmentalization based on a novel set of nuclear localization motifs.

MATERIALS AND METHODS

Plasmids. A pcDNA1 (Clontech)-based eukaryotic expression vector that encodes pyruvate kinase (Pk) with a c-*myc* epitope tag (12) at its amino terminus and a polylinker at its carboxyl terminus was used for expression studies (a gift from G. Dreyfuss, University of Pennsylvania) (45). The *myc*-Pk-NLS plasmid (a gift from M. Malim, Guy's Hospital), containing a 17-amino-acid bipartite basic NLS of hnRNP K protein (45) at the carboxy terminus of Pk has been described elsewhere (13) and was used as a positive control in expression studies. In the cases of αCP2-KL, αCP3, and αCP4A, PCR-amplified fragments corresponding to the entire coding region of respective genes or subfragments were ligated into plasmid vectors as *Xho*I-*Xba*I fragments. Given the internal *Xba*I site for αCP1 and αCP2 and compatibility between *Xba*I and *Spe*I ends, αCP1/2 full-length coding regions were cloned as *Xho*I-*Spe*I fragments into same parental vector. pB1005 (a gift from S. Smale, University of California at Los Angeles) (22), pGBD-αCP1 and pGBD-αCP2 (gifts from M. Kiledjian, Rutgers University) (30), and pET-αCP3 and pET-αCP4A were used as PCR templates to obtain a series of *myc*-tagged Pk-αCP fusion plasmids: *myc*-Pk-αCP2-KL, *myc*-Pk-αCP1, *myc*-Pk-αCP2, *myc*-Pk-αCP3, and *myc*-Pk-αCP4A, respectively. Deletion mutants of *myc*-Pk-αCP1, *myc*-Pk-αCP2, and *myc*-Pk-αCP2/KL were generated by targeted PCR. The corresponding primers contained 5′ *Xho*I site and a 3′ *Xba*I site, and the amplified fragments after restriction nuclease digestion were inserted into *myc*-Pk. Deletion mutants contained the following αCP amino acid sequences. For the N-terminal deletion series (Nd), mutants contained sequences from amino acids 17 to 331, 63 to 331, 101 to 331, 150 to 331, 257 to 331, and 306 to 331 of αCP-KL (see Fig. 4A and B) and 284 to 356 of αCP1 (see Fig. 7). For the C-terminal deletion series (Cd), mutants contained sequences from amino acids 1 to 17, 1 to 63, 1 to 101, 1 to 150, 1 to 257, and 1 to 306 of αCP2-KL (see Fig. 4C and D) and 1 to 150 of αCP1 (see Fig. 7). For the internal segment series (Is), mutants contained sequences from amino acids 150 to 256 and 257 to 306 of αCP2-KL (see Fig. 5), 151 to 290, 151 to 228, 229 to 290, 270 to 290, 280 to 290, and 270 to 279 of αCP-2 (see Fig. 6A and B), 291 to 339, 291 to 334, 318 to 339, 332 to 339, and 328 to 339 of αCP-2 (see Fig. 6C and D), and 151 to 283 of αCP-1 (see Fig. 7).

Codons encoding T at position 331 and D at position 332 of αCP2 in Pk-αCP2 were mutated by using a QuickChange kit (Stratagene) to S and G, respectively. *myc*-Pk-αCP1/ΔNLSI, *myc*-Pk-αCP2/ΔNLSI, and *myc*-Pk-αCP2/ΔNLSI/mutNLSII were constructed by spliced-overlap extension by using *myc*-Pk-αCP1, *myc*-Pk-αCP2, and *myc*-Pk-αCP2/mutNLSII as templates. Two segments of a corresponding template gene were PCR amplified independently and then fused in a subsequent reaction. The amplified fragments were inserted as *Xho*I-*Spe*I fragments into the *myc*-Pk vector.

Cell culture and transfection. HeLa cells were cultured in Dulbecco modified Eagle medium (Gibco-BRL) supplemented with 10% fetal bovine serum, 100 μg of streptomycin per ml, and 100 U of penicillin per ml. Cells were seeded into Falcon 2 chamber tissue culture glass slides (Becton Dickinson Labware, Franklin Lakes, N.J.) at a density of 1×10^5 to 2×10^5 20 h prior to transfection. Transfection of cells was performed by calcium phosphate transfection (5 Prime→3 Prime, Inc., Boulder, Colo.). Medium containing the DNA mixture was removed 18 to 20 h after transfection and replaced with fresh medium. The time when the DNA was added was considered T_0, and cells were fixed for immunofluoresence at 24 to 40 h.

Microscopy. Indirect immunofluorescence microscopy was carried out as described previously (9). After transfection, the cells were washed in 1× phosphate-buffered saline (PBS) and fixed in 1× PBS plus 3% paraformaldehyde (EM Science, Gibbstown, N.J.) for 30 min at room temperature. After fixation the cells were washed in PBS, permeabilized by the addition of 1× PBS–10% goat serum–1% Triton X-100 at room temperature for 10 min, and washed in 1× PBS. The cells were then blocked in antibody blocking-incubation buffer (ABB; 1× PBS, 10% goat serum, 0.1% Tween) for 60 min at room temperature prior to primary antibody incubation. Monoclonal anti-*myc* antibody 9E10 (Santa Cruz Biotechnology, Inc., Santa Cruz, Calif.) was then diluted 1:1,000 in ABB and applied to the cells at room temperature for 60 min. The cells were then washed and incubated with fluorescein isothiocyanate (FITC)-conjugated goat anti-mouse secondary antibody (Kirkegaard & Perry Laboratories, Gaithersburg, Md.) diluted at 1:100 in ABB for 60 min. The cells were then washed again, and glass slides were mounted with mounting medium (ProLong Antifade kit; Molecular Probes, Eugene, Oreg.) and sealed with nail polish.

For detection of endogenous αCPs and for colocalization experiments, cells were fixed in 1× PBS plus 2% paraformaldehyde for 15 min at room temperature and incubated serially with anti-αCP antibodies (FF1, FF2, and FF3) (8) and with a mouse monoclonal anti-SC35 antibody (1:150; Pharmingen, San Diego, Calif.), followed by incubation with FITC-conjugated goat anti-rabbit and Texas red (TX)-conjugated anti-mouse antibodies (1:100; Kirkegaard & Perry) in ABB for 60 min. Samples were examined by using a Leitz DMR microscope (Leica GmbH, Wetzlar, Germany), and images were captured by using a Hamamatsu color chilled 3CCD camera (model C5810; Hamamatsu Corp., Bridgewater, N.J.). Image analysis was performed by using Adobe Photoshop software (Adobe Systems, Inc., San Jose, Calif.). Optical sections were obtained by using a con-

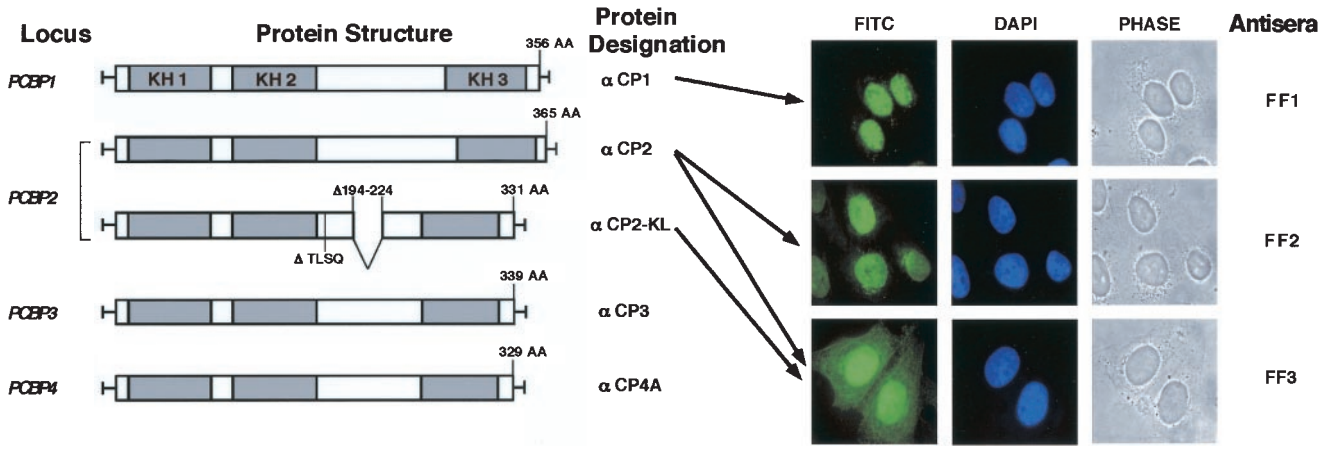

FIG. 1. αCP isoforms and detection of endogenous αCP1, αCP2, and αCP2-KL. The five major αCP isoforms are shown on the left. The corresponding genetic loci and protein designations are noted. The position of each KH domain is indicated by a shaded box. Numbers above the protein diagrams indicate the sizes of each protein in amino acids. Alternatively spliced exons are shown for the αCP2-KL. Immunostainings of HeLa cells for endogenous αCP1, αCP2, and αCP2-KL are shown on the right. The antisera are specific for αCP1 (serum FF1), αCP2 (serum FF2), and αCP2 and αCP2-KL (serum FF3). Antibody-protein complexes were visualized with FITC-conjugated goat anti-rabbit secondary antibody and examined by fluorescence microscopy. In each case the immunostained image (FITC) was compared to the nuclear stain (DAPI [4′,6′-diamidino-2-phenylindole]) and the phase-contrast image.

focal laser scanning microscope (Leica). Fluoview was operated at excitation wavelengths of 488 nm (FITC) and 568 nm (TRITC [tetramethyl rhodamine isothiocyanate]) from an argon-krypton laser. Fluorescent signals of both fluorochromes were recorded simultaneously by two detectors.

Gel electrophoresis and immunoblotting. HeLa cells were electroporated with 40 μg of plasmid DNA per 100-mm petri dish. Resuspended cells were harvested 32 h posttransfection by scraping in 0.5 ml of Laemmli sodium dodecyl sulfate sample buffer. Samples were analyzed by sodium dodecyl sulfate–12% polyacrylamide gel electrophoresis. Monoclonal anti-*myc* antibody 9E10 (Santa Cruz Biotechnology) at a 1:1,000 dilution and horseradish peroxidase-conjugated anti-mouse antibody (Boehringer Mannheim Corp., Indianapolis, Ind.) at a 1:5,000 dilution were used to detect fusion proteins, and the complexes were visualized with an enhanced chemiluminescence substrate (SuperSignal Substrate; Pierce, Rockford, Ill.).

RESULTS

αCP proteins are present in both nucleus and cytoplasm. Initial studies of αCP subcellular localization focused on the most abundantly expressed isoforms: αCP1, αCP2, and αCP2-KL (Fig. 1). HeLa cells were stained with antisera specific to αCP1 and to αCP2 (antisera FF1 and FF2, respectively) and a third antibody raised against an epitope common to αCP2 and αCP-2KL but absent from αCP1 (antisera FF3) (8). The specificities of these antisera were confirmed by Western blotting (8). In previous studies we demonstrated that the first two antisera, when used against mouse and human cell extracts, recognized a single band (αCP-1 and αCP-2, respectively), whereas the third antiserum recognized a band comigrating with αCP-2 and an additional, smaller band. The size of this additional band was consistent with that of αCP2-KL. The first two antisera (FF1 and FF2) revealed exclusive nuclear localization of αCP1 and αCP2. In contrast, the third antisera (FF3) revealed dual nuclear and cytoplasmic staining. Since full-length αCP2 is exclusively nuclear (FF2 staining), this dual-staining pattern with the FF3 antibody indicates that at least a portion of the αCP2-KL is cytoplasmic (see below for further analysis). Direct analyses of endogenous αCP3 and αCP4 isoforms were similarly attempted. However, in these two cases, the isoform-specific antisera failed to give unambiguous signals. The distributions of these proteins were addressed by detection of epitope-tagged fusion proteins (see below). We conclude from these data that the major isoforms of αCP have distinct subcellular distributions.

αCP1 is enriched in nuclear speckles. The intracellular localization of endogenous αCP1 and αCP2 were further characterized by confocal microscopy (Fig. 2). Staining with the αCP1-specific antibody revealed that the nuclear protein was

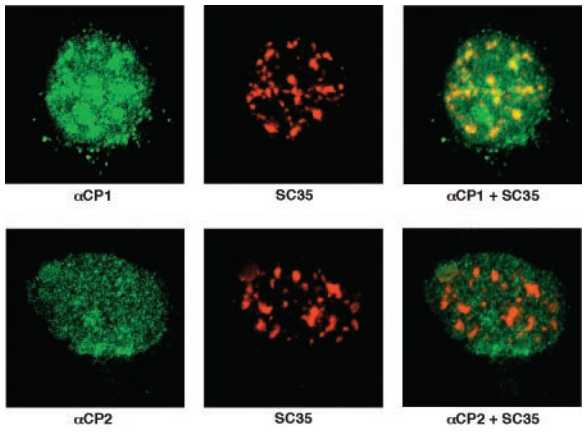

FIG. 2. Selective enrichment of αCP1 in nuclear speckles. (Top row) Localization of αCP1. HeLa cells were double immunostained with rabbit antiserum to αCP1 and mouse monoclonal antibody to SC-35. The αCP and SC35 immune complexes were detected with FITC-conjugated anti-rabbit and TX-conjugated anti-mouse antibodies, respectively, and then examined by confocal microscopy. Left panels show the αCP1 stain (FITC), middle panels show the SC35 stain (TX), and right panels show merges of the left and middle images. The yellow in the merge indicates colocalization of FITC and TX stains. (Bottom row) Localization of αCP2 (FF-2). Details are as described for the top row of images. The αCP2 is more diffusely distributed than αCP1 and does not appear to be enriched in speckles.

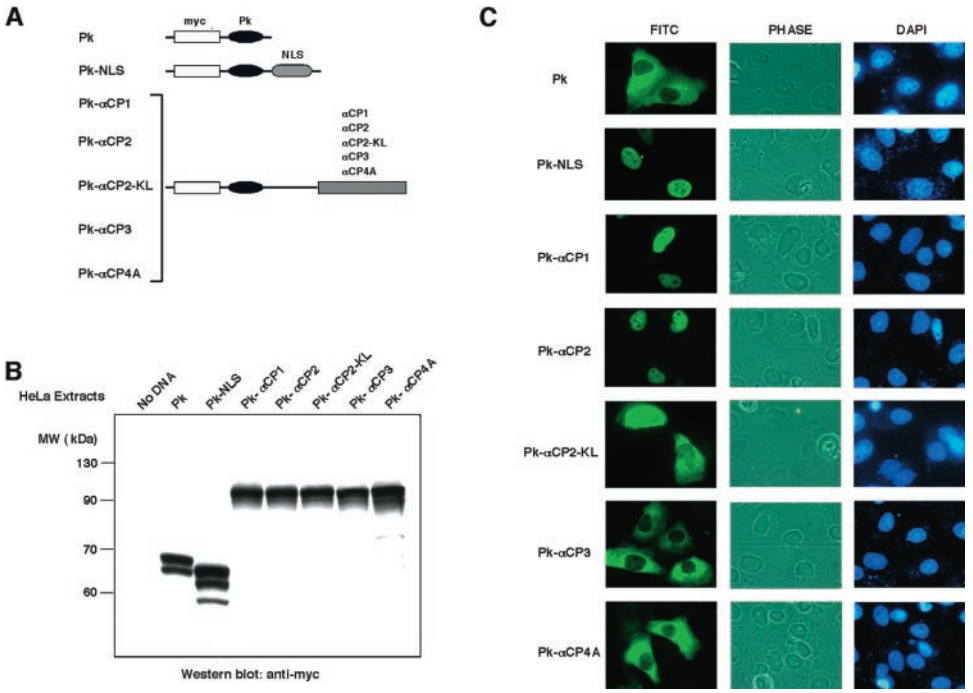

FIG. 3. Expression and subcellular localization of αCP isoforms as fusion proteins in HeLa cells. (A) Schematic drawings of the Pk-αCP isoform fusion proteins. The chicken muscle Pk (black elipse) linked to an N-terminal *myc* epitope tag (open box) was fused in a continuous ORF corresponding to each of the indicated αCP isoforms (shaded boxes). The bipartite basic NLS of hnRNP K is denoted by the stippled oval. (B) Western analysis of fusion proteins expressed in HeLa cells. Expression vectors containing each of the indicated proteins (see panel A for schematic details) were transfected into HeLa cells, and extracts were harvested at 36 h. Proteins were analyzed by Western analysis with an anti-*myc* epitope antibody (monoclonal antibody 9E10). Molecular mass standards are indicated on the left in kilodaltons. (C) Intracellular distribution of the *myc*-Pk-αCP fusion proteins. At 36 h after transfection, HeLa cells were fixed and stained for immunofluorescence microscopy with anti-*myc* antibody (FITC). Cells in the field were visualized by phase-contrast imaging, and the nuclei were identified by DAPI staining.

concentrated in clusters (Fig. 2, upper panel). These sites were consistent in size and number with nuclear speckles. To confirm this assignment, cells were double immunostained for αCP1 and splicing factor SC35 (14, 15, 73). The SC35 immunostaining revealed the same distribution as the αCP1 stain, although it was somewhat more focused. A merge of the two signals clearly demonstrated significant colocalization of αCP1 and SC35 in nuclear speckles. Confocal analysis with antisera specific to αCP2 (FF2) confirmed the nuclear-restricted pattern but, in contrast to the αCP1, the αCP2 staining was particulate and diffuse rather than speckled. Merging the αCP2 and SC35 stains failed to demonstrate significant enrichment of αCP2 in the speckles (Fig. 2, lower panel). Thus, confocal analysis confirmed the nuclear localization of αCP1 and αCP2 and revealed a selective concentration of αCP1 in nuclear speckles.

Subcellular localization of epitope-tagged αCP isoforms reveals three distribution patterns. Localization of αCP1 and αCP2 to the nucleus was unexpected since these proteins lacked identifiable nuclear import signals (53). In addition, prior studies had identified poly(C)-binding activity in cytosolic extracts (31, 80). Thus, it was likely that the cytosolic poly(C)-binding activity might reflect αCP2-KL, αCP3, and/or αCP4 content. To explore these possibilities, full-length open reading frames (ORFs) encoding each of the five major αCP isoforms were isolated and fused in frame to the ORF encoding the 55-kDa Pk and an N-terminal *myc* epitope tag (Fig. 3A). The high molecular weight of the *myc*-Pk-αCPs fusion proteins prevents nuclear entry by passive diffusion; their nuclear sublocalization should accurately reflect active transport. Control constructs included the *myc*-Pk tag alone and the myc-Pk tag fused to a known NLS. The resultant cDNAs were expressed in transfected HeLa cells. Cell extracts were analyzed by immunoblotting to confirm size, amount, and immunoreactivity of each expressed fusion protein (Fig. 3B). Localization of each fusion protein was then determined by immunostaining with a *myc* epitope monoclonal antibody (Fig. 3C). *myc*-Pk was appropriately restricted to the cytoplasm and was efficiently targeted to the nucleus when fused to the 18-amino-acid bipartite basic NLS from hnRNP K (Pk-NLS; Fig. 3C) (64). The recombinant *myc*-Pk-tagged αCP1 and αCP2 proteins were both confined to the nucleus. This was consistent with the analysis of the native proteins (Fig. 1 and 2). Analysis of the epitope-tagged αCP2-KL demonstrated that this isoform is present in both the nucleus and the cytoplasm. In contrast, the αCP3 and αCP4 fusion proteins were both confined to the cytoplasm. These data confirmed and extended the analysis of endogenous proteins and demonstrated three distinct patterns of nuclear/cytoplasmic compartmentalization: αCP1 and αCP2 are predominantly nuclear, αCP2-KL is both nuclear and cyoplasmic, and αCP3 and αCP4 are cytoplasmic.

Mapping NLSs. The αCP1, αCP2, and αCP2-KL isoforms are all present in the nucleus. However, inspection of the primary sequences failed to reveal matches with the bipartite-

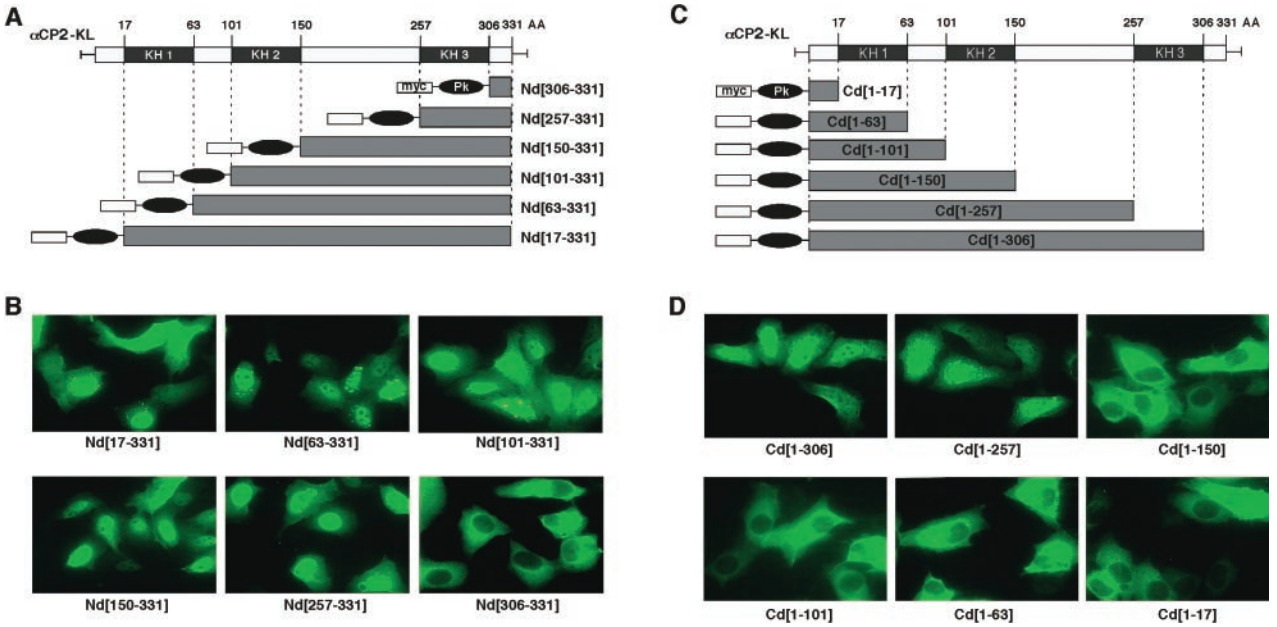

FIG. 4. Mapping nuclear import signals in αCP2-KL (A) N-terminal deletion set. The three KH domains are denoted by shaded boxes; numbers above the protein body indicate its size and the positions of KH domains in amino acids. The N and C terminus of each expressed protein is indicated along with its name. The positions of the KH domains are shown for reference. Other symbols are as defined in Fig. 3. (B) Subcellular localization of the αCP-KL Nd proteins. Representative micrographs of the immunofluorescence analyses with anti-myc are shown. The identity of each expressed protein is indicated below the frame. (C) C-terminal deletion set. Details are as described for panel A. (D) Subcellular localization of the αCP-KL Cd proteins. Details are as described for panel B.

basic or simian virus 40 large T-type NLS (11), the A1 M9 domain (45, 67), or other NLSs reported at lower frequencies (53). The sequence determinant(s) responsible for the nuclear localization therefore appeared to represent novel structures and were mapped by a functional assay (12, 13, 45). αCP2-KL was used for initial mapping since its presence in both compartments made it the most sensitive to perturbations in sorting signals. Sets of nested N-terminal and C-terminal deletions were constructed for αCP2-KL; the termini of the deletions were designed to coincide with the termini of the KH domains (Fig. 4A and C). The first N-terminal deletion [Nd(17-331)] eliminated much of the cytoplasmic accumulation seen in the native αCP2-KL but maintained the nuclear accumulation (Fig. 4B; compare with Fig. 3C). Each of the next four deletions maintained the accentuated nuclear accumulation of the fusion protein. Remarkably, nuclear localization was entirely lost subsequent to the sixth and most extensive deletion, Nd(306-331). These data suggested that there is an NLS encoded within the C-terminal 74 amino acids [Nd(257-331)]. A potential role of the extreme N terminus of αCP2 in nuclear export remains to be rigorously tested.

NLS activity was next mapped by using a reciprocal set of C-terminal deletions (Cd) of the *myc*-Pk-αCP2-KL fusion protein (Fig. 4C and D). The first two deletions failed to alter the balance of nuclear versus cytoplasmic accumulation of the αCP2-KL [Cd(1-306) and Cd(1-257)]. However, the more extensively truncated proteins localized exclusively in the cytoplasm [Cd(1-150), Cd(1-101), Cd(1-63), and Cd(1-17)], indicating that there is an NLS activity located between amino acids 150 and 257.

The combined results of the N- and C-terminal truncation sets could not be reconciled on the basis of a single NLS. The most parsimonious model comprised two separate NLSs: one located in the region between KH2 and a second located within KH3 itself. This model of two distinct NLSs was tested.

Identification of two independent NLS motifs in αCP2. Based on the results of the N-terminal and C-terminal αCP2-KL deletion studies, the regions between KH2 and KH3

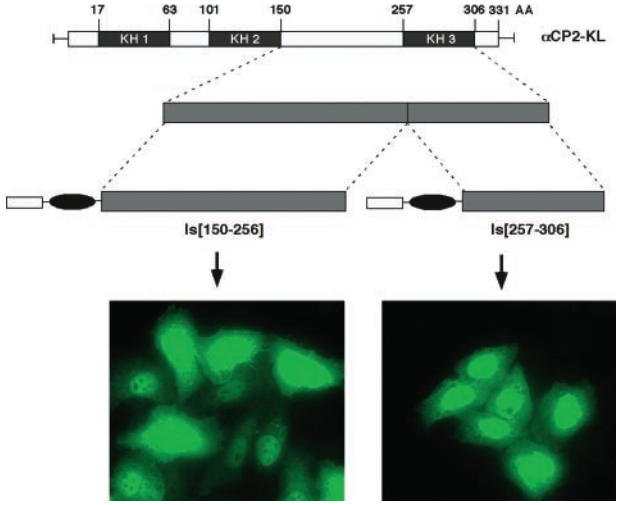

FIG. 5. αCP-2KL contains two independent NLSs. Schematics of two internal segments of the αCP2-KL fused with *myc*-Pk are shown. Immunofluorescence micrographs show the subcellular localization of the indicated αCP2-KL fusion proteins expressed in transfected HeLa cells.

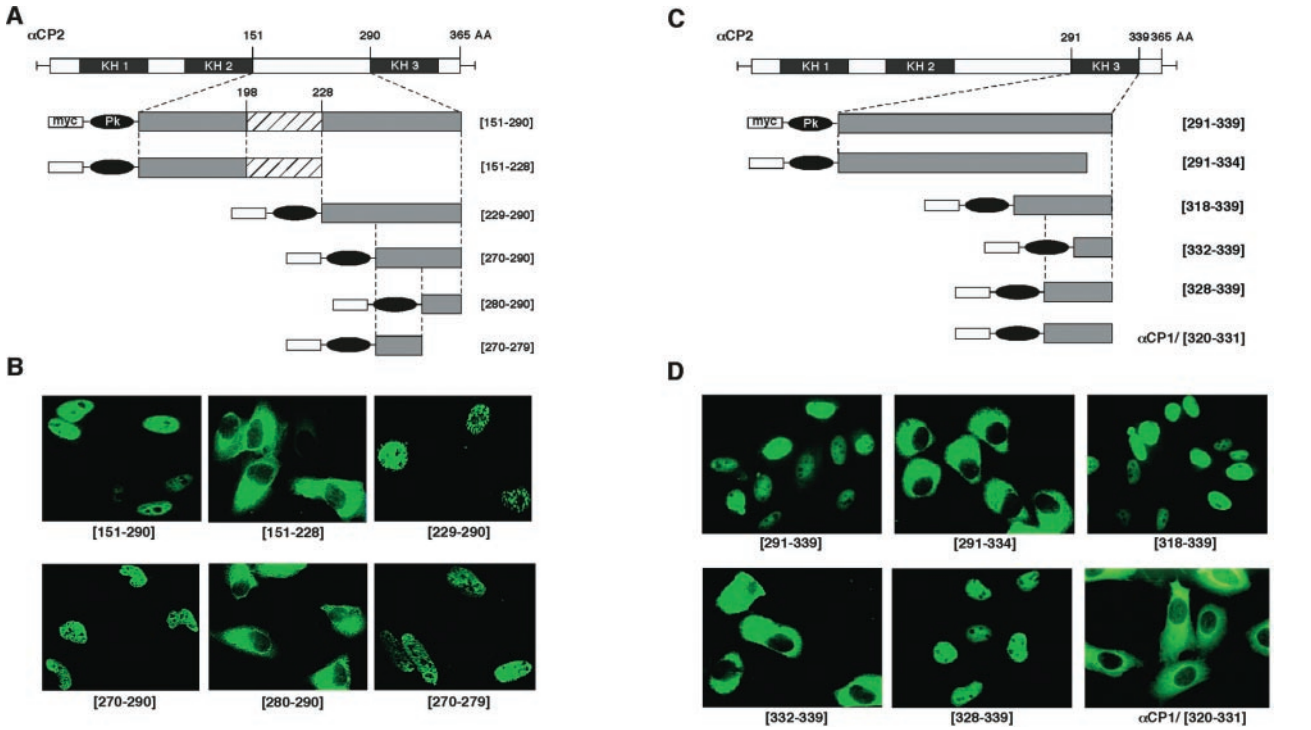

FIG. 6. Fine mapping of NLS I and NLS II. (A) Fine-mapping NLS I. Schematics of αCP2 and six subsegments assessed for NLS function. The termini of each fragment are indicated (numbers refer to the positions in the full-length αCP2). The hatch-marked box depicts a position of the additional 31-amino-acid intra-KH2/KH3 segment lacking in αCP2-KL. Each segment was fused in frame with *myc*-Pk prior to expression in HeLa cells. (B) Immunofluorescence analysis of NLS I activity. The frames show the subcellular localization of the αCP2 variants illustrated in panel A. Representative micrographs of the immunofluorescence analysis are shown. (C) Fine-mapping NLS II. Details are as described for panel A. (D) Immunofluorescence analysis of NLS II activity. Details are as described for panel B. The last inset, αCP1/[320-331], shows the subcellular localization of a *myc*-Pk fusion to the region of αCP1 corresponding to the minimal NLS II (amino acids 328 to 339) segment of αCP2 (see Fig. 7B for alignment).

[Is(150-256)] and the region encompassing KH3 through the C terminus of the αCP2-KL protein [Is(257-306)] were individually tested for NLS function (Fig. 5). The segments from amino acids 150 to 256 and amino acids 257 to 306 each individually resulted in nuclear localization of the fused *myc*-Pk reporter. These data confirmed that αCP2-KL contains at least two separable and independent NLSs: NLS I, located in the region between KH2 and KH3, and NLS II, located within the third KH domain.

Since neither NLS I nor NLS II contained a recognizable nuclear localization motif, we mapped the region between KH2 and KH3 at a higher resolution. To maximize the information from these studies, the mapping was done on αCP2 that contains the additional 31-amino-acid intra-KH2/KH3 segment lacking in αCP2-KL. A nested set of six subfragments of this region was generated (Fig. 6A). Each fragment was fused to the *myc*-Pk ORF and expressed in HeLa cells. As shown in Fig. 6B, a 10-amino-acid fragment located just N terminal to KH3 domain (i.e., from amino acids 270 to 279) was sufficient for NLS function. In a similar fashion, a set of six nested fragments representing the C terminus of the αCP2 KH3 domain were tested for NLS function (Fig. 6C). The expression patterns of these fusion proteins were sufficient to localize NLS II activity to a 12-amino-acid fragment at the C terminus of the KH3 domain (Fig. 6D). Thus, two short peptides derived from αCP2 could independently target a fusion protein to the nucleus.

Selective conservation of NLS I in αCP1. The sequences corresponding to the two NLS in αCP2 were compared to the other αCP isoforms. The sequence of NLSI in αCP2 is fully conserved in αCP1 (Fig. 7A). In contrast, the region corresponding to the αCP2 NLS II contained two divergent residues in αCP1, and even greater divergence was noted for the cytoplasmic αCP3 and αCP4 (Fig. 7B). The functional conservation of NLS motifs in αCP1 was tested. αCP1 was divided into three segments (Fig. 8A). Each segment was fused to *myc*-Pk, and the distribution of the expressed protein was determined in transfected cells (Fig. 8B). The fragment encompassing the region between KH2 and KH3, Is(151-283), directed recombinant protein transport to the nucleus. In contrast, the fragment encompassing KH3 and the C terminus, Nd(284-356), lacked NLS function. To clarify the functional impact of these two amino acid substitutions on NLS II function, the αCP1 peptide corresponding to NLS II was directly tested by fusing it to the *myc*-Pk reporter. The expressed fusion protein was limited to the cytoplasm (Fig. 6C and D). Similarly, the corresponding regions of αCP3, αCP4, and hnRNP K (Fig. 7B) were all incapable of directing *myc*-Pk reporter to nucleus (data not shown). These data demonstrate that αCP1 carries a single NLS (NLS I) and that αCP2 and αCP2-KL contain two inde-

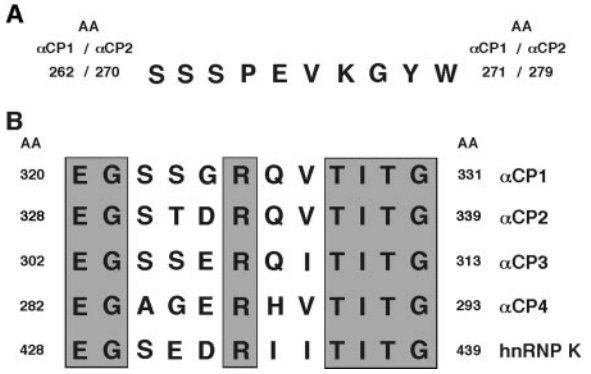

FIG. 7. Sequence alignments of major αCP isoforms at NLS I and NLS II. (A) Alignment of the sequences corresponding to NLS I. This alignment shows perfect conservation between αCP1 and αCP2. There is no region presented in αCP3 or αCP4 that has significant homology to this sequence. (B) Alignments of the sequences corresponding to NLS II. These alignments reveal divergence among αCP2, the other αCP isoforms, and hnRNP K. Conserved amino acids are shaded.

pendently functioning NLSs (NLS I and NLS II). In contrast, αCP3 and αCP4 lack effective NLS determinants.

NLS I and NLS II function as essential transport determinants in their native context. The mapping studies presented above demonstrate that NLS I and NLS II are each sufficient to translocate the *myc*-Pk reporter to the nucleus. The function of these determinants was next tested in the context of the full-length αCP1 and αCP2 proteins (Fig. 9). NLS I (amino acids 262 to 271) was deleted from αCP1 (Fig. 9A). The resulting *myc*-Pk fusion protein, αCP1/ΔNLS I, was restricted to the cytoplasm of transfected HeLa cells (Fig. 9B). Thus, deletion of NLS I resulted in the loss of nuclear accumulation.

To determine whether one or both of the NLSs are necessary for nuclear localization of αCP2, they were inactivated separately and in combination (Fig. 9C). *myc*-Pk-αCP2/ΔNLSI encoded an αCP2 lacking the NLS I (residues 270 to 279). *myc*-Pk-αCP2/mutNLSII contains two amino acid substitutions at positions 331 (T-S) and 332 (D-G) that inactivate NLS II function (Fig. 8). The third recombinant, *myc*-Pk-αCP2/ΔNLSI/mutNLSII, lacks both NLSs. Each protein was expressed in HeLa cells (Fig. 9D). As expected, *myc*-Pk-αCP2 localized exclusively in the nucleus. Deletion of NLS I (*myc*-Pk-αCP2/ΔNLSI) resulted in some redistribution of the protein to the cytoplasm, but it was not sufficient in the context of the otherwise-intact αCP2 to fully block nuclear localization. Mutation of NLS II alone (*myc*-Pk-αCP2/mutNLSII) also caused some redistribution of the protein to the cytoplasm, although the majority of the protein remained in the nucleus. In contrast, the combined inactivation of both NLS I and NLS II (*myc*-Pk-αCP2/ΔNLSI/mutNLSII) resulted in exclusive redistribution of αCP2 to the cytoplasm. These observations indicate that the single NLS I is both necessary and sufficient for the nuclear localization of αCP1, whereas two distinct NLSs are present in αCP2 and appear to play redundant roles in protein transport.

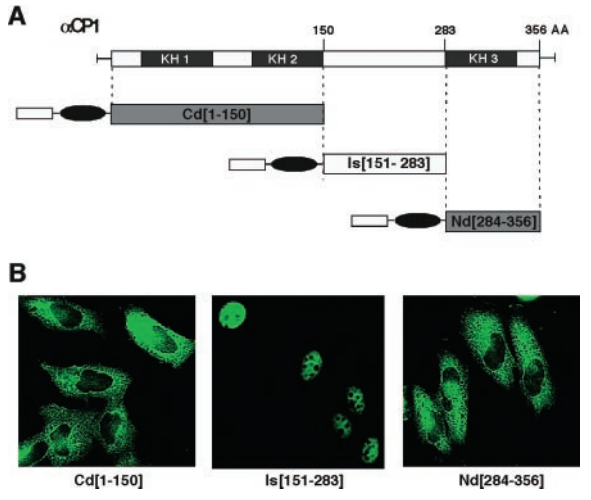

FIG. 8. NLS activity in αCP1 is restricted to the region between KH2 and KH3. (A) Division of αCP1 into three segments for NLS mapping. The termini of each segment are noted. (B) Immunofluorescence analysis of the αCP1 subregions. *myc*-Pk-tagged αCP1 subregions were expressed in HeLa cells, and the subcellular distribution of each protein was determined. Representative micrographs of the immunofluorescence analysis are shown.

DISCUSSION

αCPs comprise a highly abundant subset of RNA-binding proteins. The four dispersed *PCBP* loci encode five distinct αCP isoforms. These proteins play prominent roles in post-transcriptional control of cellular and viral mRNAs. To what extent αCP isoforms overlap in functions and/or mediate specific controls is now under study. As a step in this direction, we have defined the intracellular localizations of five major αCP isoforms. In the process of these studies, we have identified a novel set of NLSs that contribute their respective distributions.

αCP1 and αCP2 localize predominantly to the nucleus. This conclusion is based on immunofluorescence analysis of endogenous proteins with isoform-specific antisera, as well as epitope-tagged fusion proteins expressed in cells. The nuclear localization of these two αCP isoforms can be compared to two prior data sets. In one study, mCBP (mouse homolog of αCP2) appeared to be predominantly nuclear (17), whereas a second study reported cytoplasmic localization of PCBP1 (αCP1) and PCBP2 (αCP2) (18). Our present data agree with the first study. To try to clarify the discrepancy with the second cited study, we repeated analyses by using the fixation technique, cells, and staining protocols specified in that study, including the use of the same antibody preparations (gifts from R. Andino). Despite these efforts, we were unable to resolve the conflicting data since αCP1 and αCP2 were consistently detected only in the nuclear compartment.

Although both αCP1 and αCP2 are localized to the nucleus, their respective distributions are not identical. αCP1 is selectively concentrated in nuclear speckles, whereas αCP2 is more diffusely distributed (Fig. 2). Speckles, or interchromatin granule clusters (IGCs) (reviewed in references 33 and 70), represent sites at which splicing factors are concentrated prior to assembly on newly synthesized transcripts (26, 29, 48). Recently, Mintz et al. biochemically purified IGCs. Consistent with the present study, αCP1 was specifically identified as one of 75 IGC-associated proteins (47). Association of other αCP isoforms with IGCs was not observed. On the other hand,

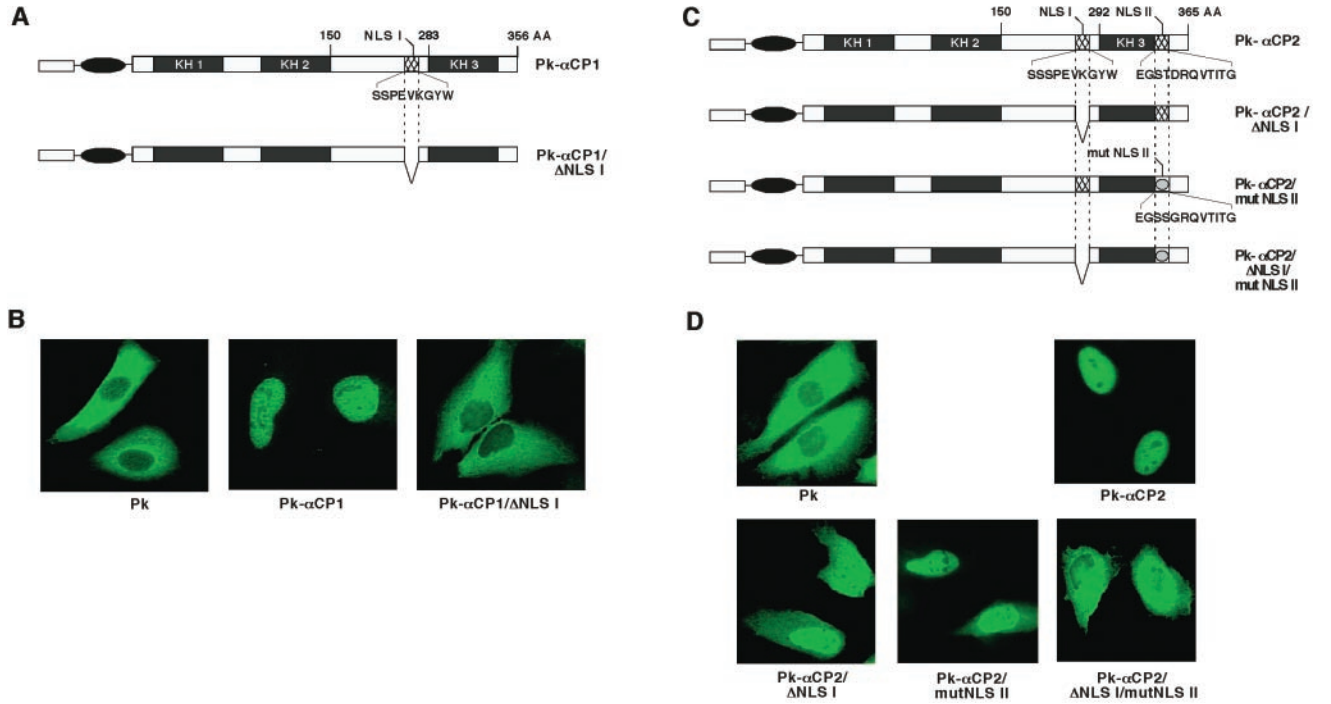

FIG. 9. Nuclear localization of the full-length αCP1 and αCP2 proteins is dependent on defined set of novel NLSs. (A) Schematic of wild-type *myc*-Pk-αCP1 and the mutant lacking NLS I (*myc*-Pk-αCP1/ΔNLSI). The cross-hatched box represents NLS I. The primary sequence of NLS I is shown. (B) Immunofluorescence micrographs showing the subcellular localization of wild-type and NLSI-deleted αCP1 proteins. Plasmids encoding *myc*-Pk-αCP1 and *myc*-Pk-αCP1/ΔNLSI proteins were transfected into HeLa cells, and the subcellular distribution of the proteins was determined. Representative micrographs of the immunofluorescence analysis are shown. (C) Schematic of wild-type αCP2 and the mutants lacking one or both of NLS I and NLS II. A schematic of wild-type *myc*-Pk-αCP2 and three derivative mutants in which NLS I, NLS II, or NLS I plus NLS II were inactivated (*myc*-Pk-αCP2/ΔNLSI, *myc*-Pk-αCP2/mutNLSII, and *myc*-Pk-αCP2/ΔNLSI/mutNLSII, respectively) is shown. The two cross-hatched boxes represent NLS I and NLS II. The position of deleted NLS I is indicated by the gap, and the boxes with ovals depict the mutated NLS II. (D) Immunofluorescence micrographs showing the subcellular localization of the wild-type αCP2 and the derivative NLS mutants. Plasmids encoding *myc*-Pk-tagged αCP2, *myc*-Pk-αCP2/ΔNLSI, *myc*-Pk-αCP2/mutNLSII, and *myc*-Pk-αCP2/ΔNLSI/mutNLSII were transfected into HeLa cells, and the subcellular distribution of the proteins was determined. Representative micrographs of the immunofluorescence analysis are shown.

Funke et al. presented evidence for in vivo interaction between αCP2-KL and splicing factor 9G8 (17). We were not able to detect convincing data that support a selective enrichment of αCP2/αCP2-KL in speckles. Although it is possible that the interaction with 9G8 occurs outside of speckles, further studies are needed to clarify this issue. The localization of αCP1 to nuclear speckles raises the possibility that this particular αCP isoform has a role in pre-mRNA splicing. This function is supported by the recent finding that interference with nuclear αCP activity via targeted RNA decoys blocks efficient splicing of the hα-globin transcript (D. Eastmond, J. Kong, and S. A. Liebhaber, unpublished data). Thus, nuclear localization and the function of αCPs is supported by a number of lines of evidence and is strengthened by the current data set.

The structural basis for the distinct subcellular compartmentalization of the various αCP isoforms is undoubtedly complex. The present study focuses on determinants of αCP nuclear localization. Two functional NLSs were identified in αCP2, and one of these is conserved in αCP1. Remarkably, the newly identified NLS I and NLS II have no apparent similarity to each other and bear little or no resemblance to NLSs described in the literature. Specifically, they lack similarity to either the bipartite-basic type or the simian virus 40 large T-type NLSs or to shuttling signals found in hnRNP A1 (45, 67), hnRNP K (46), HuR (16, 62), and human immunodeficiency virus type 1 Rev (44, 71). Protein basic local alignment search tool (BLAST) (1) searches optimized for searching for small sequences (i.e., 1, "search for short nearly exact matches," matrix PAM30; gap penalties: existence, 9; extension, 1) failed to identify other proteins with significant primary sequence homology. Although it is unlikely that these two NLSs are unique to the αCPs, they do appear to be uncommon. The presence of two independent NLSs in one protein is not unprecedented. As an example, hnRNP K contains a classical NLS at the N-terminal end and KNS (i.e., hnRNP K nuclear shuttling domain) between the KH2 and KH3 RNA-binding domains (46). It is interesting that hnRNP K does not contain the two NLSs in the closely related αCP1 and αCP2 (Fig. 7).

NLSs can be grouped on the basis of both transport pathways and structure. A subset of NLSs described in the literature demonstrates transcription-dependent transport activity (45, 67, 81). To determine whether the NLSs found in αCP1 and αCP2 fall in this functional category, we transfected cells with *myc*-Pk-tagged αCPs and then treated the cells with either actinomycin D or 5,6-dichlororibofuranosylbenzimidazole (DRB). These treatments failed to result in any change in

intracellular localization of the endogenous or epitope-tagged αCP1 or αCP2 (data not shown). In addition, the identified NLS I and NLS II sequences do not match to the previously described importin-α and importin-β recognition signals (23, 60, 76). It remains to be determined whether the apparently novel NLSs of αCP1 and αCP2 represent noncanonical binding sites of the currently known transport receptors, or whether they interact with novel factors of the intracellular transport.

The distribution of αCP2-KL in both nuclear and cytoplasmic compartments is of particular interest because this protein comprises the major αCP isoform in certain cell types (8, 38, 39). The structure of the nuclear αCP2 differs from that of αCP2-KL by the inclusion of a 31-amino-acid alternatively spliced segment located between the KH2 and KH3 RNA-binding domains (see Fig. 1). It is formally possible that this 31-amino-acid segment encodes an additional NLS. However, this appears unlikely since this isolated segment is unable to localize a fused *myc*-Pk to the nucleus (Fig. 6B). A more plausible model would be that this segment encodes a nuclear retention signal that anchors αCP2 in the nucleus. The presence of a nuclear retention signal in hnRNP C proteins establishes a precedent for this model (52).

Visual examination of the αCP amino acid sequences reveals a candidate N-terminal Leu-rich motif between that may serve a direct nuclear export function. Although we observed that its deletion shifted αCP2-KL localization to the nuclear compartment (Fig. 4A and B), the direct role of this sequence in intracellular trafficking of αCP proteins remains to be fully tested. The presence of nuclear export signal and NLS motifs in αCP1 and αCP2 would support a shuttling activity of these proteins (see below).

The colocalization of NLS II with the KH3 RNA-binding domain of αCP2 suggests a possible interplay between RNA-binding domain and subcellular transport. αCP2 may initially bind to target mRNAs in the nucleus during transcription and/or processing. An initial association of αCPs with target mRNAs in the nucleus is supported by the recent finding that expression of RNA decoys to αCP selectively in the nucleus results in a block in both nuclear (splicing) and cytoplasmic (translation and stabilization) activities (40; Eastmond et al., unpublished). Binding of αCP to a target mRNA in the nucleus may block NLS II which is located within an RNA-binding (KH) domain. This might facilitate redistribution of the αCP-RNP complex to the cytoplasm because both NLS I and NLS II are needed for efficient nuclear localization (Fig. 9). Once in the cytoplasm, the cytoplasmic function(s) of the αCP2-RNP complex can be achieved; the αCP2 may then dissociate from the cytoplasmic mRNA. The newly exposed NLS II, in conjunction with NLS I, could then mediate efficient reimportation of αCP2/2-KL to the nucleus. A similar model of RNP cycling via reversible NLS function has been suggested for HIV Rev (23). The proposed reversible RNA association of αCPs with target mRNAs may be further facilitated by posttranscriptional modifications (34). αCP may thus bind to a target mRNA in the nucleus, facilitate mRNP export, have an impact on cytoplasmic control over mRNA stability and/or translation, and then return to the nucleus. Given the present delineation of αCP localization and underlying NLS motifs, these models can now be further explored.

ACKNOWLEDGMENTS

We thank R. Andino, G. Dreyfuss, and M. Malim for generously sharing reagents used in this study. We thank Julia Morales for early contributions to this project, Brian Calvi for advice on confocal microscopy, and Lili Wan for critical review of the manuscript.

This work was supported by NIH grant RO1 HL65449 and by the generosity of the Doris Duke Foundation.

REFERENCES

1. **Altschul, S. F., T. L. Madden, A. Schaffer, J. Zhang, Z. Zhang, W. Miller, and D. J. Lipman.** 1997. Gapped BLAST and PSI-BLAST: a new generation of protein database search programs. Nucleic Acids Res. **25:**3389–3402.
2. **Andino, R., N. Boddeker, D. Silvera, and A. Gamarnik.** 1999. Intracellular determinants of picornavirus replication. Trends Microbiol. **7:**76–82.
3. **Belsham, G. J., and N. Sonenberg.** 2000. Picornavirus RNA translation: roles for cellular proteins. Trends Microbiol. **8:**330–335.
4. **Biamonti, G., and S. Riva.** 1994. New insights into the auxiliary domains of eukariotic RNA binding proteins. FEBS Lett. **340:**1–8.
5. **Buckanovich, R. J., and R. B. Darnell.** 1997. The neuronal RNA binding protein Nova-1 recognizes specific RNA targets in vitro and in vivo. Mol. Cell. Biol. **17:**3194–3201.
6. **Burd, C. G., and G. Dreyfuss.** 1994. Conserved structures and diversity of functions of RNA-binding proteins. Science **265:**615–621.
7. **Canete-Soler, R., and W. W. Schlaepfer.** 2000. Similar poly(C)-sensitive RNA-binding complexes regulate the stability of the heavy and light neurofilament mRNAs. Brain Res. **867:**265–279.
8. **Chkheidze, A. N., D. L. Lyakhov, A. V. Makeyev, J. Morales, J. Kong, and S. A. Liebhaber.** 1999. Assembly of α-globin mRNA stability complex reflects binary interaction between the pyrimidine-rich 3′ untranslated region determinant and poly(C) binding protein αCP. Mol. Cell. Biol. **19:**4572–4581.
9. **Choi, Y. D., and G. Dreyfuss.** 1984. Isolation of the heterogeneous nuclear RNA ribonucleoprotein complex (hnRNP): a unique supramolecular assembly. Proc. Natl. Acad. Sci. USA **81:**7471–7475.
10. **Czyzyk-Krzeska, M. F., and A. C. Bendixen.** 1999. Identification of the poly(C) binding protein in the complex associated with the 3′ untranslated region of erythropoietin messenger RNA. Blood **93:**2111–2120.
11. **Dingwell, C., and R. A. Laskey.** 1991. Nuclear targeting sequences: a consensus? Trends Biochem. Sci. **16:**478–481.
12. **Evan, G., G. Lewis, G. Ramsay, and J. M. Bishop.** 1985. Isolation of monoclonal antibodies specific for human c-muc proto-oncogene product. Mol. Cell. Biol. **5:**3610–3616.
13. **Fouchier, R. A., B. E. Meyer, J. H. Simon, U. Fischer, and M. H. Malim.** 1997. HIV-1 infection of non-dividing cells: evidence that the amino-terminal basic region of the viral matrix protein is important for Gag processing but not for post-entry nuclear import. EMBO J. **16:**4531–4539.
14. **Fu, X.-D., and T. Maniatis.** 1990. Factor required for mammalian spliceosome assembly is localized to discrete regions in the nucleus. Nature **343:** 437–441.
15. **Fu, X.-D., and T. Maniatis.** 1992. Isolation of a complementary DNA that encodes the mammalian splicing factor SC35. Science **256:**535–538.
16. **Fun, X. C., and J. A. Steitz.** 1998. HNS, a nuclear-cytoplasmic shuttling sequence in HuR. Proc. Natl. Acad. Sci. USA **95:**15293–15298.
17. **Funke, B., B. Zuleger, R. Benavente, T. Schuster, M. Goller, J. Stevenin, and I. Horak.** 1996. The mouse poly(C)-binding protein exists in multiple isoforms and interacts with several RNA-binding proteins. Nucleic Acids Res. **24:**3821–3828.
18. **Gamarnik, A., and R. Andino.** 1997. Two functional complexes formed by KH domain containing proteins with the 5′ noncoding region of poliovirus RNA. RNA **3:**882–892.
19. **Gorlich, D., and U. Kutay.** 1999. Transport between the cell nucleus and the cytoplasm. Annu. Rev. Cell Dev. Biol. **15:**607–660.
20. **Gorlich, D., and I. W. Mattaj.** 1996. Nucleocytoplasmic transport. Science **271:**1513–1518.
21. **Grishin, N. Y.** 2001. KH domain: one motif, two folds. Nucleic Acids Res. **29:**638–643.
22. **Hahm, K., G. Kim, C. W. Turck, and S. T. Smale.** 1993. Isolation of a murine gene encoding a nucleic acid-binding protein with homology to hnRNP K. Nucleic Acids Res. **21:**3894.
23. **Handerson, B. R., and P. Percipalle.** 1997. Interactions between HIV Rev and nuclear import and export factors: the Rev nuclear localization signal mediates specific binding to human importin-β. J. Mol. Biol. **274:**693–707.
24. **Hazelrigg, T.** 1998. The destinies and destinations of RNAs. Cell **95:**451–460.
25. **Holcik, M., and S. A. Liebhaber.** 1997. Four highly stable eukaryotic mRNAs assemble 3′ untranslated region RNA-protein complexes sharing *cis* and *trans* components. Proc. Natl. Acad. Sci. USA **94:**2410–2414.
26. **Huang, S., and D. L. Spector.** 1996. Intron-dependent recruitment of pre-mRNA splicing factors to sites of transcription. J. Cell Biol. **133:**719–732.
27. **Jensen, K. B., K. Musunuru, H. A. Lewis, S. K. Burley, and R. B. Darnell.** 2000. The tetranucleotide UCAY directs the specific recognition of RNA by the Nova K-homology 3 domain. Proc. Natl. Acad. Sci. USA **97:**5740–5745.

28. **Ji, X., J. Kong, and S. A. Liebhaber.** 2003. In vivo association of the stability control protein αCP with actively translating mRNAs. Mol. Cell. Biol. **23:** 899–907.
29. **Jimenez-Garcia, L. F., and D. L. Spector.** 1993. In vivo evidence that transcription and splicing are coordinated by a recruiting mechanism. Cell **73:** 47–59.
30. **Kiledjian, M., C. T. DeMaria, G. Brewer, and K. Novick.** 1997. Identification of AUF1 (heterogeneous nuclear ribonucleoprotein D) as a component of the alpha-globin mRNA stability complex. Mol. Cell. Biol. **17:**4870–4876.
31. **Kiledjian, M., X. Wang, and S. A. Liebhaber.** 1995. Identification of two KH domain proteins in the α-globin mRNA stability complex. EMBO J. **14:** 4357–4364.
32. **Kong, J., X. Ji, and S. A. Liebhaber.** 2003. The KH-domain protein αCP has a direct role in mRNA stabilization independent of its cognate binding site. Mol. Cell. Biol. **23:**1125–1134.
33. **Lamond, A. I., and W. C. Earnshaw.** 1998. Structure and function in the nucleus. Science **280:**547–553.
34. **Leffers, H., K. Dejgaard, and J. E. Celis.** 1995. Characterization of two major cellular poly(C)-binding human proteins, each containing three K-homologous (KH) domains. Eur. J. Biochem. **230:**447–453.
35. **Lewis, H. A., H. Chen, C. Edo, R. J. Buckanovich, Y. Y. Yang, K. Musunuru, R. Zhong, R. B. Darnell, and S. K. Burley.** 1999. Crystal structures of Nova-1 and Nova-2 K-homology RNA-binding domains: structure with folding and design. Structure **7:**191–203.
36. **Lewis, H. A., K. Musunuru, K. B. Jensen, C. Edo, H. Chen, R. B. Darnell, and S. K. Burley.** 2000. Sequence-specific RNA binding by a Nova KH domain: implications for paraneoplastic disease and the fragile X syndrome. Cell **100:**323–332.
37. **Liebhaber, S. A.** 1997. mRNA stability and the control of gene expression. Nucleic Acids Symp. Ser. **36:**29–32.
38. **Makeyev, A. V., A. N. Chkheidze, and S. A. Liebhaber.** 1999. A set of highly conserved RNA-binding proteins, αCP1 and αCP2, implicated in mRNA stabilization, are coexpressed from an intronless gene and its intron-containing paralog. J. Biol. Chem. **274:**24849–24857.
39. **Makeyev, A. V., and S. A. Liebhaber.** 2000. Identification of two novel mammalian genes establishes a subfamily of KH-domain RNA-binding proteins. Genomics **67:**301–316.
40. **Makeyev, A. V., D. L. Eastmond, and S. A. Liebhaber.** 2002. Targeting a KH-domain protein with RNA decoys. RNA **8:**1160–1173.
41. **Makeyev, A. V., and S. A. Liebhaber.** 2002. The poly(C)-binding proteins: a multiplicity of function and a search for mechanisms. RNA **8:**265–278.
42. **Mattaj, I. W., and L. Englmeier.** 1998. Nucleocytoplasmic transport: the soluble phase. Annu. Rev. Biochem. **67:**265–306.
43. **Matunis, M. J., W. M. Michael, and G. Dreyfuss.** 1992. Characterization and primary structure of the poly(C)-binding heterogeneous nuclear ribonucleoprotein complex K protein. Mol. Cell. Biol. **12:**164–171.
44. **Meyer, B. E., and M. H. Malim.** 1994. The HIV-1 Rev transactivator shuttles between the nucleus and the cytoplasm. Genes Dev. **8:**1538–1547.
45. **Michael, W. M., M. Choi, and G. Dreyfuss.** 1995. A nuclear export signal in hnRNP A1: a signal-mediated, temperature-dependent nuclear protein export pathway. Cell **83:**415–422.
46. **Michael, W. M., P. S. Eder, and G. Dreyfuss.** 1997. The K nuclear shuttling domain: a novel signal for nuclear import and nuclear export in the hnRNP K protein. EMBO J. **16:**3587–3598.
47. **Mintz, P. J., S. D. Patterson, A. F. Neuwald, C. S. Spahr, and D. L. Spector.** 1999. Purification and biochemical characterization of interchromatin granule clusters. EMBO J. **18:**4308–4320.
48. **Misteli, T., J. F. Caceres, and D. L. Spector.** 1997. The dynamics of a pre-mRNA splicing factor in living cells. Nature **387:**523–527.
49. **Morales, J., J. E. Russell, and S. A. Liebhaber.** 1996. Destabilization of human α-globin mRNA by translation anti-termination is controlled during erythroid differentiation and is paralleled by phased shortening of the poly(A) tail. J. Biol. Chem. **272:**6607–6613.
50. **Musco, G., A. Kharrat, G. Stier, F. Fraternali, T. J. Gibson, M. Nilges, and A. Pastore.** 1997. The solution structure of the first KH domain of FMR1, the protein responsible for the fragile X syndrome. Nat. Struct. Biol. **4:**712–716.
51. **Musco, G., G. Stier, C. Joseph, M. A. Castiglione Morelli, M. Nilges, T. J. Gibson, and A. Pastore.** 1996. Three-dimensional structure and stability of the KH domain: molecular insights into the fragile X syndrome. Cell **85:** 237–245.
52. **Nakielny, S., and G. Dreyfuss.** 1996. The hnRNP C protein contain a nuclear retention sequence that can override nuclear export signals. J. Cell Biol. **134:**1365–1373.
53. **Nakielny, S., and G. Dreyfuss.** 1999. Transport of proteins and RNAs in and out of the nucleus. Cell **99:**677–690.
54. **Nigg, E. A.** 1997. Nucleocytoplasmic transport: signals, mechanisms and regulation. Nature **386:**779–787.
55. **Ohno, M., M. Fornerod, and I. W. Mattaj.** 1998. Nucleocytoplasmic transport: the last 200 nanometers. Cell **92:**327–336.
56. **Ostareck-Lederer, A., D. H. Ostareck, and M. W. Hentze.** 1998. Cytoplasmic regulatory functions of the KH-domain proteins hnRNPs K and E1/E2. Trends Biochem. Sci. **23:**409–411.
57. **Ostareck, D. H., A. Ostareck-Lederer, I. N. Shatsky, and M. W. Hentze.** 2001. Lipoxygenase mRNA silencing in erythroid differentiation: the 3′UTR regulatory complex controls 60S ribosomal subunit joining. Cell **104:**281–290.
58. **Ostareck, D. H., A. Ostareck-Lederer, M. Wilm, B. J. Thiele, M. Mann, and M. W. Hentze.** 1997. mRNA silencing in erythroid differentiation: hnRNP K and hnRNP E1 regulate 15-lipoxygenase translation from the 3′ end. Cell **89:**597–606.
59. **Paillard, L., D. Maniey, P. Lachaume, V. Legagneux, and H. B. Osborne.** 2000. Identification of a C-rich element as a novel cytoplasmic polyadenylation element in *Xenopus* embryos. Mech. Dev. **93:**117–125.
60. **Palmeri, D., and M. H. Malim.** 1999. Importin beta can mediate the nuclear import of an arginine-rich nuclear localization signal in the absence of importin alpha. Mol. Cell. Biol. **19:**1218–1225.
61. **Paulding, W. R., and M. F. Czyzyk-Krzeska.** 1999. Regulation of tyrosine hydroxylase mRNA stability by protein-binding, pyrimidine-rich sequence in the 3′-untranslated region. J. Biol. Chem. **274:**2532–2538.
62. **Peng, S. S., C. Y. Chen, N. Xu, and A. B. Shyu.** 1998. RNA stabilization by the AU-rich element binding protein, HuR, an ELAV protein. EMBO J. **17:**3461–3470.
63. **Perrotti, D., V. Cesi, R. Trotta, C. Guerzoni, G. Santilli, K. Cmpbell, A. Iervolino, F. Condorelli, C. Gambacorti-Passerini, M. A. Caligiuri, and B. Calabretta.** 2002. BCR-ABL suppresses C/EBPa expression through inhibitory action of hnRNP E2. Nat. Genet. **30:**48–58.
64. **Richardson, W. D., B. L. Roberts, and A. E. Smith.** 1986. Nuclear location signals in polyoma virus large T. Cell **44:**77–85.
65. **Ross, J.** 1995. mRNA stability in mammalian cells. Microbiol. Rev. **59:**423–450.
66. **Silvera, D., A. V. Gamarnik, and R. Andino.** 1999. The N-terminal K homology domain of the poly(rC)-binding protein is a major determinant for binding to the poliovirus 5′-untranslated region and acts as an inhibitor of viral translation. J. Biol. Chem. **274:**38163–38170.
67. **Siomi, H., and G. Dreyfuss.** 1995. A nuclear localization domain in the hnRNP A1 protein. J. Cell Biol. **129:**551–560.
68. **Siomi, H., and G. Dreyfuss.** 1997. RNA-binding proteins as regulators of gene expression. Curr. Opin. Genet. Dev. **7:**345–353.
69. **Siomi, H., M. J. Matunis, W. M. Michael, and G. Dreyfuss.** 1993. The pre-mRNA binding K protein contains a novel evolutionarily conserved motif. Nucleic Acids Res. **21:**1193–1198.
70. **Spector, D. L.** 1993. Macromolecular domains within the cell nucleus. Annu. Rev. Cell Biol. **9:**265–315.
71. **Stauber, R., A. S. Gaitanaris, and G. N. Pavlakis.** 1995. Analysis of trafficking of Rev and transdominant Rev proteins in living cells using green fluorescent protein fusions: transdominant Rev blocks the export of Rev from the nucleus to the cytoplasm. Virology **213:**126–136.
72. **Stefanovic, B., C. Hellerbrand, M. Holcik, M. Briendl, S. Liebhaber, and D. A. Brenner.** 1997. Posttranscriptional regulation of collagen alpha1(I) mRNA in hepatic stellate cells. Mol. Cell. Biol. **17:**5201–5209.
73. **Sukegawa, J., and G. Blobel.** 1995. A putative mammalian RNA helicase with an arginine-serine-rich domain colocalizes with a splicing factor. J. Biol. Chem. **270:**15702–15706.
74. **Thisted, T., D. L. Lyakhov, and S. Liebhaber.** 2001. Optimized RNA targets of two closely related triple KH domain proteins, heterogeneous nuclear ribonucleoprotein K and αCP-2KL, suggest distinct modes of RNA recognition. J. Biol. Chem. **276:**17484–17496.
75. **Tommerup, N., and H. Leffers.** 1996. Assignment of human KH-box-containing genes by in situ hybridization: HNRNPK maps to 9q21.32-q21.33, PCBP1 to 2p12-p13, and PCBP2 to 12q13.12-q13.13, distal to FRA12A. Genomics **32:**297–298.
76. **Truant, R., and B. R. Cullen.** 1999. The arginine-rich domains present in human immunodeficiency virus type 1 Tat and Rev function as direct importin beta-dependent nuclear localization signals. Mol. Cell. Biol. **19:**1210–1217.
77. **Vasu, S. K., and D. J. Forbes.** 2001. Nuclear pores and nuclear assembly. Curr. Opin. Cell Biol. **13:**363–375.
78. **Wang, Z., N. Day, P. Trifillis, and M. Kiledjian.** 1999. An mRNA stability complex functions with poly(A)-binding protein to stabilize mRNA in vitro. Mol. Cell. Biol. **19:**4552–4560.
79. **Wang, Z., and M. Kiledjian.** 2000. Identification of an erythroid-enriched endoribonuclease activity involved in specific mRNA cleavage. EMBO J. **19:**295–305.
80. **Wang, X., M. Kiledjian, I. M. Weiss, and S. A. Liebhaber.** 1995. Detection and characterization of a 3′ untranslated region ribonucleoprotein complex associated with human α-globin mRNA stability. Mol. Cell. Biol. **15:**1769–1777.
81. **Weighardt, F., G. Biamonti, and S. Riva.** 1995. Nucleo-cytoplasmic distribution of human hnRNP proteins: a search for the targeting domains in the hnRNP A1. J. Cell Sci. **108:**545–555.
82. **Weiss, I. M., and S. A. Liebhaber.** 1994. Erythroid cell-specific determinants of α-globin mRNA stability. Mol. Cell. Biol. **14:**8123–8132.

83. **Weiss, I. M., and S. A. Liebhaber.** 1995. Erythroid cell-specific mRNA stability elements in the α2-globin 3′ nontranslated region. Mol. Cell. Biol. **15:**2457–2465.
84. **Xiao, X., Y. S. Tang, J. Y. Mackins, X. L. Sun, H. N. Jayaram, D. K. Hansen, and A. C. Antony.** 2001. Isolation and characterization of a folate receptor mRNA-binding trans-factor from human placenta: evidence favoring identity with heterogeneous nuclear ribonucleoprotein E1. J. Biol. Chem. **276:** 41510–41517.
85. **Yeap, B. B., D. C. Voon, J. P. Vivian, R. K. McCulloch, A. M. Thomson, K. M. Giles, M. F. Czyzyk-Krzeska, H. Fuurneaux, M. C. J. Wilce, J. A. Wilce, and P. J. Leedman.** 2002. Novel binding of HuR and poly[copy]-binding proteins to a conserved UC-rich motif within the 3′-untranslated region of the androgen receptor messenger RNA. J. Biol. Chem. **277:**27183–27192.
86. **Yu, J., and J. E. Russell.** 2001. Structural and functional analysis of an mRNP complex that mediates the high stability of human β-globin mRNA. Mol. Cell. Biol. **21:**5879–5888.